Available online at www.sciencedirect.com
ScienceDirect
Journal of Nuclear Materials 373 (2008) 328–334
journal of nuclear materials
www.elsevier.com/locate/jnucmat

Neutron irradiation effect on site distribution of cations in non-stoichiometric magnesium aluminate spinel

Takashi Sawabe *, Toyohiko Yano

Research Laboratory for Nuclear Reactors, Tokyo Institute of Technology, 2-12-1 O-okayama, Meguro-ku, Tokyo 152-8550, Japan

Received 21 October 2006; accepted 21 June 2007

Abstract

Neutron irradiation effects on cation distribution in non-stoichiometric Mg–Al spinel were examined by ALCHEMI (Atom Location by Channeling Enhanced Microanalysis) method. Parameter n, or non-stoichiometry of $MgO \cdot nAl_2O_3$ of the specimens, were $n = 1.00$, 1.01, 1.10, 1.48. These specimens were neutron-irradiated up to a fluence of 2.3×10^{24} n/m^2 ($E > 0.1$ MeV) at 500–530 °C in JMTR. Some specimens contracted by the irradiation and the arrangement of cations became more disorder. The other specimens showed very small swelling by the irradiation and the cation distribution became slightly ordered. The cation distribution of the contracted specimen returned stepwise to the pre-irradiated condition after the annealing at 700 °C. The cation distribution of the slightly swollen specimens did not change after the annealing up to 700 °C. Cation distribution in the T-site was more sensitively influenced by the irradiation.

PACS: 61.50.Nw; 61.66.Fn; 61.80.Hg; 61.85.+p

1. Introduction

Magnesium aluminate spinel crystallizes in the isometric system with an octahedral habit. The general chemical formula is as $A^{2+}B_2^{3+}O_4^{2-}$, with A representing a divalent cation (Mg^{2+}) and B a trivalent cation (Al^{3+}). The oxygen anions are arranged in the cubic closest-packed structure. There are 32 octahedral interstices, 16 of which are occupied by trivalent cations (O-site). The divalent cations are located at eight of the 64 tetrahedral interstices (T-site). The remaining interstices, which are called as structural vacancies, are unoccupied in natural spinel but have the capability to accommodate cation species within a stable structure at high temperature and pressure [1]. The physical and structural properties of magnesium aluminate spinel vary according to the following factors: lattice parameter (a), anion parameter (u, which is a measure of the oxygen dilation) and cation inversion parameter (x) [2]. The general chemical formula is shown as $(A_{1-x}B_x)[A_xB_{2-x}]O_4$ with the parameter x. For normal spinel, $x = 0$; for random spinel, $x = 2/3$; and for inverse spinel, $x = 1$. Natural, or mineral, $MgAl_2O_4$ spinel exhibits approximately the normal spinel-structure, so that $x \approx 0$; but synthetic Mg–Al spinels exhibit cation distribution between tetrahedral and octahedral sites [3].

The degree of cation distribution in spinel has been determined by various methods such as IR (infrared spectroscopy) [4] and Raman spectroscopy [5–7], NMR (nuclear magnetic resonance) [3,8–10], calorimetric measurements [11,12], neutron diffraction [13,14], and ALCHEMI (atom location by channeling enhanced microanalysis) [15].

On the other hand, spinel exhibits a wide range of non-stoichiometry, and it is denoted as $MgO \cdot nAl_2O_3$. The value of n in $MgO \cdot nAl_2O_3$ ranges from <0.6 to >7 at $\sim$1990 °C [16]. As n increases, the lattice parameter decreases from $a = 0.8078$ nm for $n = 1.0$ to 0.7964 nm for $n = 3.5$ composition [17]. In non-stoichiometric spinel, Al cations are substituted for Mg cations accompany with formation of cation vacancies (unoccupied sites) to

* Corresponding author. Tel.: +81 3 5734 3082; fax: +81 3 5734 3082.
E-mail address: 06d19012@nr.titech.ac.jp (T. Sawabe).

0022-3115/$ - see front matter © 2007 Published by Elsevier B.V.
doi:10.1016/j.jnucmat.2007.06.013

maintain charge neutrality. Chemical formula of non-stoichiometric spinel can be shown as $Vc_{(n-1)/(3n+1)}Mg_{4/(3n+1)}Al_{8n/(3n+1)}O_4$, where Vc represents cation vacancy.

It is well-known that spinel shows superior radiation resistance against a very severe fast neutron irradiation. Spinel exhibits very small swelling by neutron irradiation [18–24], and the strength and toughness of spinel are increased [19,25–29]. The reason for radiation resistance has been attributed to difficulty of loop nucleation and unfaulting dislocation loops [30–34]. Most of the point defects generated during irradiation probably annihilate by interstitial-vacancy recombination [30–32,35]. The interstitial-vacancy recombination in irradiated spinel was confirmed as inducement of cation relocation which was measured by neutron diffraction [35], NMR [36] and ALCHEMI technique [15].

There are a limited number of systematic studies of irradiation effect for non-stoichiometric spinel, particularly the effect of thermal annealing on recovery of defects. Parker et al. reported that faulted loops appeared with $\mathbf{b} = a/4\langle 1\,1\,0\rangle$ on $\{1\,1\,0\}$ planes in the $n = 1$ and 1.1 spinels, and with $\mathbf{b} = a/6\langle 1\,1\,1\rangle$ on $\{1\,1\,1\}$ planes in the $n = 1.1$ and 2 spinels [32]. Soeda et al. measured the site distribution of cations in spinels with different n, and the non-stoichiometric spinel showed more resistance to radiation damage than the stoichiometric one [15]. One of the present authors reported changes in macroscopic length, lattice parameter, Vickers hardness and thermal diffusivity of spinel ceramics with different compositions [22–24]. Macroscopic length of some of the near-stoichiometric spinels reduced by the neutron irradiation (2.3×10^{24} n/m at 500–530 °C) and they returned to the pre-irradiation value by the annealing at around 650 °C [23]. These studies clarified that the irradiation effects of near-stoichiometric spinels were different from ones of non-stoichiometric spinels. Since reasons for these differences are not clear, then the extended studies in irradiated $MgO \cdot nAl_2O_3$ spinels are necessary to understand the role of non-stoichiometry. In this study, spinel specimens with four compositions ($n =$ 1.00, 1.01, 1.10, 1.48) whose irradiation condition was the same as our previous study [23] were concurrently irradiated by fast neutrons. Cation distribution of the specimens was examined by ALCHEMI to clarify the neutron irradiation effect and subsequent annealing effect in these specimens. Then the mechanism of those irradiation effects was elucidated from the viewpoint of the cation distribution.

2. Theory

The technique of ALCHEMI, which was proposed by Spence and Taftø [37–39], enables the fraction of impurity atoms on a given host-site in the crystal. It is determined from ratios of characteristic X-ray count rates at various crystal orientations. Spinel-structure compounds can be separated into alternating (4 0 0) planes of tetrahedral site (T-site) and octahedral site (O-site) in the [0 0 1] projection. In the 'ideal' stoichiometric spinel, Mg cations occupy only T-site and Al cations occupy only O-site. Cation occupancy in natural spinel is nearly equivalent to the ideal case, but in synthetic spinel, part of Mg and Al cations occupy O-site and T-site, respectively [7,35,40].

Let $N_i^{(\zeta)}$ be the characteristic X-ray intensity from the element i for the two incident beam orientation (ζ). X-ray intensity is shown as Eq. (1). $I_T^{(\zeta)}$ and $I_O^{(\zeta)}$ are the thickness averaged electron intensities on the T-site and O-site, respectively. P_i is the ratio of the element i in the T-site to the whole element i, and K_i is a factor that accounts for fluorescence yield and other scaling factors

$$N_i^{(\zeta)} = K_i\left\{I_T^{(\zeta)}P_i + I_O^{(1\zeta)}(1-P_i)\right\}. \tag{1}$$

Channeling orientation is $\zeta = 1$. The X-ray intensities from the element Mg and Al in spinel are shown as

$$\begin{aligned} N_{Al}^{(1)} &= K_{Al}\{I_T^{(1)}P_{Al} + I_O^{(1)}(1-P_{Al})\},\\ N_{Mg}^{(1)} &= K_{Mg}\{I_T^{(1)}P_{Mg} + I_O^{(1)}(1-P_{Mg})\}. \end{aligned} \tag{2}$$

Non-channeling orientation is $\zeta = 2$, which makes $I_T^{(2)} = I_O^{(2)} = I$. The X-ray intensities on the non-channeling condition are shown as

$$\begin{aligned} N_{Mg}^{(2)} &= K_{Mg}I,\\ N_{Al}^{(2)} &= K_{Al}I. \end{aligned} \tag{3}$$

Then, we obtain the relation Eq. (4) using Eqs. (2) and (3)

$$\begin{aligned} \frac{N_{Mg}^{(1)}}{N_{Mg}^{(2)}} &= \frac{I_T^{(1)}}{I}P_{Mg} + \frac{I_O^{(1)}}{I}(1-P_{Mg}),\\ \frac{N_{Al}^{(1)}}{N_{Al}^{(2)}} &= \frac{I_T^{(1)}}{I}P_{Al} + \frac{I_O^{(1)}}{I}(1-P_{Al}). \end{aligned} \tag{4}$$

Thus, the parameter P_{Mg} and P_{Al} can be found if $I_T^{(1)}/I$ and $I_O^{(1)}/I$ can be found. The cation distribution of stoichiometric spinel was expressed as $Mg_{1-x}Al_x(Mg_xAl_{2-x})O_4$. The relations of P_{Mg}, P_{Al} and x are $P_{Mg} = 1 - x$ and $P_{Al} = x/2$ in the case of stoichiometric spinel. The measured x values in natural spinel ranged within 0–0.06 at room-temperature [14,35,40,41]. In the case of $x = 0$, no cation substitution occurs and corresponds to the ideal cation distribution. The value of $x = 0.06$ indicates slight disordering.

P_{Mg} and P_{Al} were calculated on the three assumptions (a), (b) and (c). (a) Cations are not in structural vacancies in natural spinel but they are allowed staying in structural vacancies in synthetic spinels and irradiated spinels. (b) Al cation had 97.3% ideal cation distribution ($1 - P_{Al} =$ 0.973) in natural spinel, which is based on the previous report ($x = 0.054$) by Kashii et al. [1]. (c) One Mg cation in T-site displaces one Al cation in O-site in natural spinel because of (a). Then, $P_{Mg} = 0.946$ and $P_{Al} = 0.027$ were calculated by (a) and (b). $I_T^{(1)}/I$, $I_O^{(1)}/I$ can be found from Eq. (4). And unknown P_i of the other samples can be found by the analysis data, $I_T^{(1)}/I$, $I_O^{(1)}/I$ and Eq. (4). Shortage of cation occupancies from the ideal occupancies in the

Table 1
Macroscopic length change and lattice parameter change of spinels after neutron irradiation (2.3×10^{-24} n/m^2 ($E>0.1$ MeV) at 500–530 °C in Japan Materials Testing Reactor)

Composition	Specimen ID	Macroscopic length change (%)	Lattice parameter change (%)
$n=1.00$	6	−0.040	−0.045
	7	0.004	0.006
	8	−0.052	−0.041
	10	−0.072	−0.068
$n=1.01$	40	0.000	0.006
	41	0.004	−0.004
	42	0.008	0.009
	43	0.004	Not obtained
	44	−0.035	−0.046
$n=1.10$	75	0.015	0.006
	76	0.008	−0.007
	78	0.000	−0.004
	79	0.000	0.007
$n=1.48$	111	0.019	−0.006
	112	0.004	−0.020
	113	0.008	−0.015
	114	0.008	−0.009

Ref. [23].

T- and O-sites attributed as cation vacancies. Excess is attributed as structural vacancies.

Currently, effects of strain induced by irradiation are considered to affect the electron channeling behavior because those irradiation effects deform channeling planes. On condition of this experiment, the macroscopic length change and the lattice parameter change of spinel specimens were very small due to the formation of only point defects (Table 1) [23]. Furthermore, we could not observe the formation of radiation-induced dislocations in the present specimens which were irradiated lower neutron fluence than the loop formation fluence [30–34]. Therefore, the change in diffraction condition due to the irradiation on electron channeling behavior is considered to be negligible.

3. Experimental procedures

The specimens were a natural spinel crystal (Mogok, Myanmar) for the standard, and synthetic polycrystalline spinels with different compositions ($MgO\cdot nAl_2O_3$, $n=1.00$, 1.01, 1.10, 1.48). The polycrystalline spinels were irradiated with fast neutrons up to 2.3×10^{24} n/m^2 ($E>0.1$ MeV) (estimated roughly as ~0.2 dpa) at 500–530 °C in the Japan Materials Testing Reactor using a He-filled temperature controlled rig [22]. After the neutron irradiation, the macroscopic length change and the lattice parameter change of these specimens were investigated previously by one of the present authors (Table 1) [23]. The average length change and corresponding lattice parameter change by the irradiation were very small, but some specimens contracted relatively large amount. We chose specimens; ID40 ($n=1.01$), ID44 ($n=1.01$), ID78 ($n=1.10$) and ID113 ($n=1.48$) for ALCHEMI experiment. ID44 was the contracted specimen.

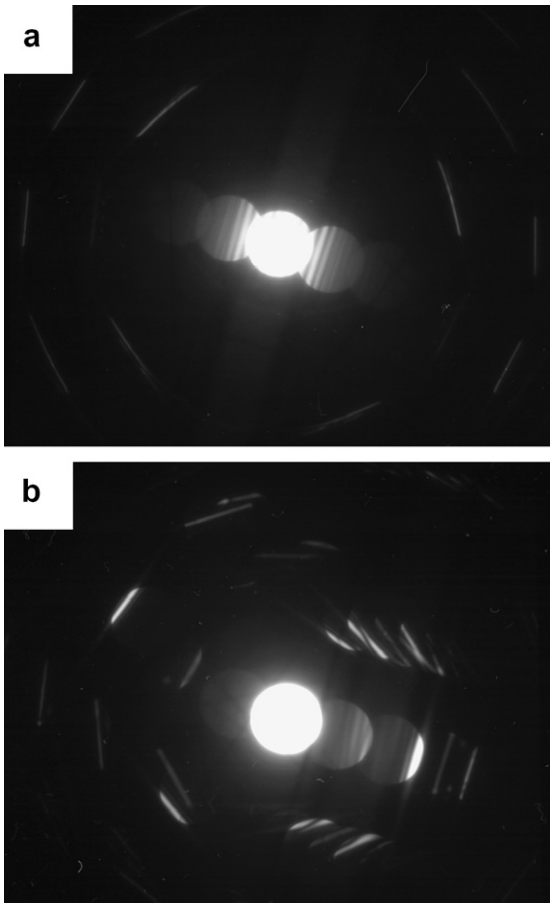

Fig. 1. Electron diffraction patterns corresponding to $0g_{400}$ Bragg condition (a) and $4g_{400}$ Bragg condition (b).

The foils for TEM observation and analysis were prepared by ion milling method. ALCHEMI experiment was performed using a Hitachi H-9000, furnished with a KEVEX Delta III ultra thin window type EDS detector. The data were acquired at an accelerating voltage of 300 kV with an electron probe about 0.75 μm in diameter. The specimen was tilted into the $[h\,0\,0]$ systematic orientation around the [0 0 1] zone axis. The spectra were recorded at $0g_{4\,0\,0}$ and $4g_{4\,0\,0}$ Bragg conditions (Fig. 1) at each orientation from the regions of 80–160 nm in thickness. Total acquired signals of Mg and Al characteristic X-rays were around ~10000 counts. The thickness was measured by convergent beam electron diffraction (CBED) contrast. Next, each thin foil specimen was isochronally annealed using an infrared heating furnace at 400–800 °C for 1 h, then the data were acquired as described above.

4. Results

This paper addresses cation occupancy as the ratio of cations in own ideal host-site to the whole cations, in other words Mg cation occupancy (T-site) is P_{Mg} and Al cation

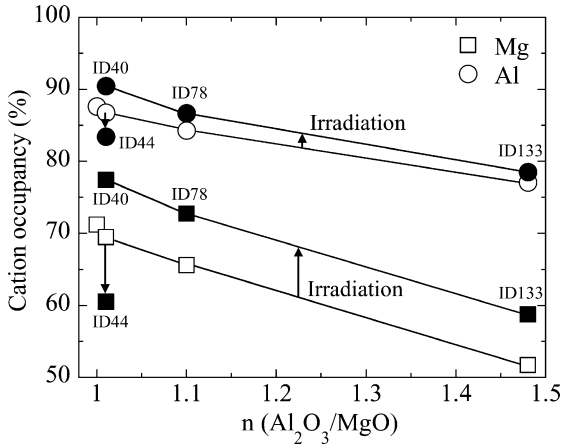

Fig. 2. Cation occupancy of the T-site and O-site of the spinel specimens with different n before (open marks) and after neutron irradiation (closed marks).

occupancy (O-site) is $1 - P_{Al}$. The cation occupancies of the unirradiated $MgO \cdot nAl_2O_3$ specimens as a function of parameter n are shown in Fig. 2. Cations in the synthetic specimens were less ordered than the cations in the natural spinel, whose cation occupancies were smaller than those of the natural spinel. The larger n value of the specimens, the more random occupancy of the cation was in the unirradiated specimens. Both Al occupancy in octahedral site (O-site) and Mg occupancy in tetrahedral site (T-site) decreased with increase in n. The irradiated specimens ID40, 78 and 113, showed similar tendency with those of unirradiated specimens, and the cation occupancies decreased with increasing n. It is noted that the cations in the irradiated specimens except ID44 were slightly ordered than before the neutron irradiation, otherwise the cations in ID44 were disordered more.

The distribution of cations and cation vacancies in the unit cell of spinel was calculated. The calculation results about pre-irradiated specimens are shown in Table 2. Minus figures indicate 'excess occupancy in structural vacancy'. 'Cation vacancy' and 'structural vacancy' of T-site or O-site are on the same channeling plane in this analysis, so that they are not distinguished. Or, cations in 'cation vacancy' and in 'structural vacancy', which are on the same channeling plane, are obtained same signal. We can find that cations were combined with either T-site or O-site, but we cannot find this combination either 'cation vacancy' or 'structural vacancy'. Therefore, we have considered that cations combine with 'cation vacancies' first due to requirement of charge neutrality in an ionic crystal. Next they combine with 'structural vacancies' if there are no 'cation vacancies' on that site. Recombination of knocked-on cations is also considered as described above. Tables 2–4 are based on this assumption.

Table 2
Cation and vacancy distribution in T-site and O-site of unirradiated spinel specimens

n		T-site (8)	O-site (16)	Total
1.00	Mg	5.70	2.30	8.00
	Al	1.98	14.02	16.00
	Vacancy	0.32	−0.32[a]	0.00
1.01	Mg	5.52	2.42	7.94
	Al	2.12	13.92	16.04
	Vacancy	0.36	−0.34[a]	0.02
1.10	Mg	4.88	2.56	7.44
	Al	2.57	13.80	16.37
	Vacancy	0.55	−0.36[a]	0.19
1.48	Mg	3.04	2.84	5.88
	Al	3.99	13.42	17.41
	Vacancy	0.97	−0.26[a]	0.71

[a] Minus figures indicate 'excess occupancy in structural vacancy'.

Table 3
Cation and vacancy distribution in T-site and O-site of irradiated spinel specimens

Specimen ID		T-site (8)	O-site (16)	Total
40	Mg	6.15	1.79	7.94
	Al	1.53	14.51	16.04
	Vacancy	0.32	−0.30[a]	0.02
44	Mg	4.80	3.14	7.94
	Al	2.66	13.38	16.04
	Vacancy	0.54	−0.52[a]	0.02
78	Mg	5.41	2.03	7.44
	Al	2.18	14.19	16.37
	Vacancy	0.41	−0.22[a]	0.19
113	Mg	3.46	2.42	5.88
	Al	3.74	13.67	17.41
	Vacancy	0.80	−0.09[a]	0.71

[a] Minus figures indicate 'excess occupancy in structural vacancy'.

Table 4
Effect of annealing on change in the cation and vacancy distribution in T-site and O-site on the irradiation specimen ID44, measured at room-temperature

Annealing temperature (°C)		T-site (8)	O-site (16)	Total
20	Mg	4.80	3.14	7.94
	Al	2.66	13.38	16.04
	Vacancy	0.54	−0.52[a]	0.02
400	Mg	4.73	3.21	7.94
	Al	2.74	13.30	16.04
	Vacancy	0.53	−0.51[a]	0.02
500	Mg	4.77	3.17	7.94
	Al	2.79	13.25	16.04
	Vacancy	0.44	−0.42[a]	0.02
600	Mg	4.80	3.14	7.94
	Al	2.82	13.22	16.04
	Vacancy	0.38	−0.36[a]	0.02
700	Mg	5.59	2.35	7.94
	Al	2.19	13.85	16.04
	Vacancy	0.22	−0.20[a]	0.02
800	Mg	5.66	2.28	7.94
	Al	2.01	14.03	16.04
	Vacancy	0.33	−0.31[a]	0.02

[a] Minus figures indicate 'excess occupancy in structural vacancy'.

The number of Al cations in the T-site increased when the parameter n increases. Inversely, the number of Mg cations in the T-site decreased. It was interesting that the number of cations in the host-site (in the case of Mg, the T-site) decreased when the parameter n increased. Furthermore, most of cation vacancies were located in the T-site.

The cation and vacancy distribution of the irradiated spinel are shown in Table 3. Mg cations in the T-site and Al cations in the O-site of the specimens ID40 ($n = 1.01$), ID78 ($n = 1.10$) and ID113 ($n = 1.48$) increased by the neutron irradiation. The concentration of cation vacancies in the T-site slightly decreased by the neutron irradiation. On the other hand, Mg cations in the T-site and Al cations in the O-site of the specimen ID44 ($n = 1.01$) decreased. Cation vacancies were more concentrated in the T-site.

The changes of the cation occupancy in the natural spinel with increasing isochronal annealing temperature are plotted in Figs. 3 and 4. The changes of the cation occupancy in both T-site and O-site were small. The cation occupancy of the irradiated specimens ID40, ID78 and ID113 with increasing post-irradiation isochronal annealing temperature changed also small, thus no clear change was observed between 400 and 700 °C.

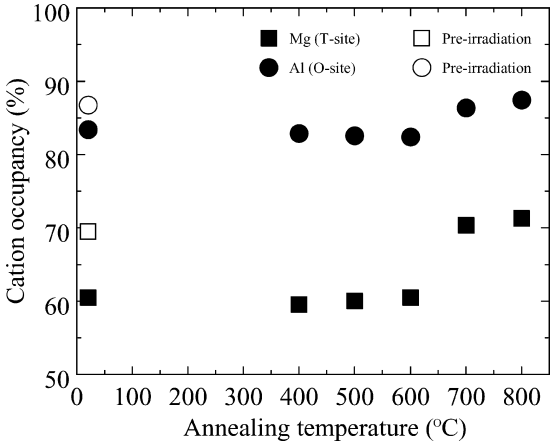

Fig. 5. Changes in cation occupancy of Mg in the T-site and Al in the O-site of the irradiated specimen ($n = 1.01$:ID44, closed marks) with increasing annealing temperature. Open marks are these of unirradiated specimen.

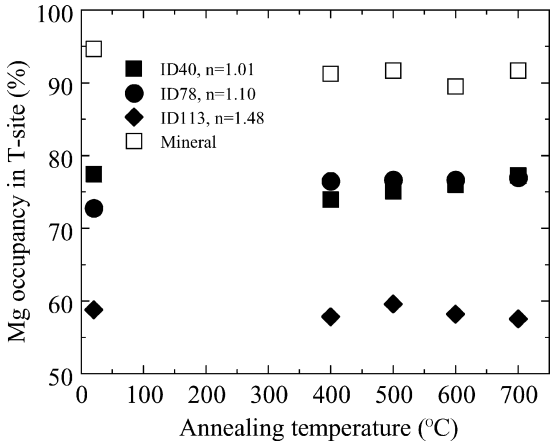

Fig. 3. Change in cation occupancy of Mg in the T-site of the irradiated specimen ($n = 1.01$:ID40, $n = 1.10$:ID78, $n = 1.48$:ID113) and that of unirradiated mineral specimen with increasing annealing temperature.

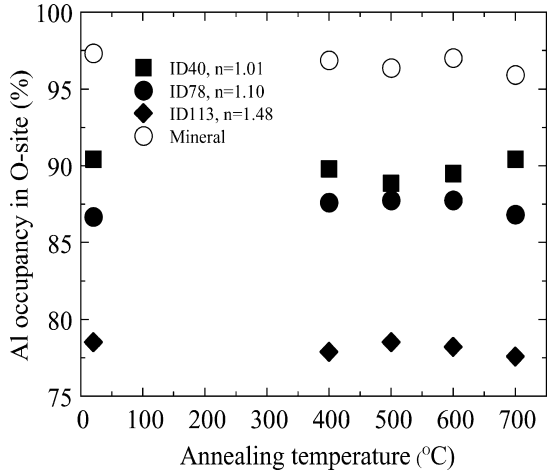

Fig. 4. Change in cation occupancy of Al in the O-site of the irradiated specimen ($n = 1.01$:ID40, $n = 1.10$:ID78, $n = 1.48$:ID113) and that of unirradiated mineral specimen with increasing annealing temperature.

Fig. 5 indicates the change of the cation occupancy in the irradiated specimen ID44 with increasing post-irradiation isochronal annealing temperature. The cation occupancy below 600 °C was not shown any changes. Above this temperature, both Mg occupancy in the T-site and Al occupancy in the O-site showed a stepwise increase in the temperature range of 600–700 °C. The calculated cation and vacancy distribution with increasing annealing temperature about the specimen ID44 is shown in Table 4. It is worthy noted that the amount of recovery at 700 °C coincided well with the amount of disorder due to the neutron irradiation.

5. Discussion

5.1. Effect of non-stoichiometry

Spinel-structure compounds are typical ionic crystals. Cation distribution in them is determined mainly by electrostatic potential and ionic radius. These compounds are generally normal-type spinel (AB_2O_4) when the radius of A cation is smaller than the radius of B cation. Some compounds are inverse-type spinel ($B(AB)O_4$) when the radius of A cation is larger than the radius of B cation. However, it is known that this rule does not always true. In $MgAl_2O_4$, the radius of Mg^{2+} is larger than the radius of Al^{3+}. The structure is supposed to be inverse-type spinel based on the rule, but it is normal-type spinel, practically.

It was clarified from Fig. 2 and Table 2 that the disordering of cations in unirradiated non-stoichiometric spinel was larger with an increase in parameter n. Total number

of Al cation in the unit cell increased with an increased in parameter n. On the contrary, number of Al cation in host-site (O-site) decreased gradually. In parallel, total number of Mg cation in the unit cell decreased and number of Mg cation in anti-host-site (O-site) increased i.e., number of Mg cation in host-site (T-site) decreased with increasing n. T-site is enlarged by including Mg cation because the original space of T-site is smaller for Mg cation. The upper limit of the tetrahedral enlargement is the point, where two O anions come in contact with each other. The size of tetrahedron is restricted by the relation of lattice parameter and ionic radii, so that allowance of the enlargement to include Mg cation in T-site decrease with decrease in lattice parameter. As parameter n increases, lattice parameter decreases [17]. The smaller allowance in the larger n spinel caused the number of Mg cation in the host-site to decrease. On the other hand, the cation vacancies, which are generated for maintaining charge neutrality if the value of n is larger than unity, concentrated only in the T-site (Table 2). The distribution of cation vacancies might contribute to reduce average size of the T-site.

5.2. Effect of irradiation

The cation distribution of the present specimens showed two kinds of changes due to the neutron irradiation (Fig. 2 and Table 3). The specimens ID40, 78 and 113 were ordered, and the specimen ID44 was disordered by the neutron irradiation.

In the case of the specimens ID40, 78 and 113, the disordering of cations after the neutron irradiation was lager with an increase in parameter n as in the case of non-irradiated specimens, but the cation distribution of each specimen was found to become order by the irradiation. This result indicates that numbers of knocked-on cations were recombined preferentially with cation or structural vacancies of those host-sites (Mg: T-site, Al: O-site). The concentration of cation vacancies in the T-site was reduced by the neutron irradiation and the O-site was fully occupied. The knocked-on cations were mainly recombined with cation vacancies in the T-site. Our present result agrees well with the result of the study performed by Soeda et al. [15].

In the case of the specimen ID44, Table 3 shows that knocked-on cations were recombined more with the anti-site cation or structural vacancies. Then, the lattice parameter of the specimen ID44 reduced relatively large amount by the neutron irradiation [23], as can be seen in Table 1. These results were coincided with the previous studies [41–43], namely the lattice parameter decreases with increasing the inversion parameter x. The enlargement of T-site by including Mg cation might reduce because the number of Mg cation in T-site decreased by the neutron irradiation. Thus, we conclude that the reduction of the average size of tetrahedron was the reason for the reduction of the lattice parameter or the macroscopic length of the specimen ID44 reducing.

5.3. Effect of annealing

The cation occupancy in the natural spinel showed small change after annealing up to 700 °C (Figs. 3 and 4). Then, the effect of the anneal treatment up to 700 °C on cation occupancy was negligible in the unirradiated spinel. As shown in Fig. 5, the cation occupancy in the specimen ID44 showed stepwise recovery to the pre-irradiation occupancy after the annealing at 700 °C. It is reported that the order–disorder phase transition in Mg–Al spinel is observed at 650–700 °C [41]. It is therefore that the recovery for post-irradiation annealing in the specimen ID44 was attributed to the order–disorder phase transition of Mg–Al spinel. The total number of the cations in the O-site in the post-irradiated ID44 specimen was 16.52, then cations were over-packed into the O-site (Table 3). Thus, over-plus cations may be located in the interstitial O-site where no atom exists in the case of ideal structure (structural vacancy). As mentioned in the introduction, 16 of 32 O-sites are occupied in ideal structure. If the over-plus cations occupy vacant octahedral sites, the cation-occupied octahedron shared edges with surrounding octahedron, and density of cations increases markedly in this area. Then, it is reasonable to assume that the cations in the interstitial O-site were less stable than that in the ordinary O-site, originally cation-occupied position. A part of cations can migrate at 700 °C, above the order–disorder transition temperature, and then they recombined with cation vacancies. During the order–disorder phase transition, Mg and Al cations occupy the pre-irradiation positions in average, as a result excess cations in the O-site reduced, as shown in Table 4.

The cation occupancy in the specimens ID40, 78 and 113 changed little during annealing compared with the pre-irradiated occupancy. Annealing caused almost no occupancy change, as shown in Figs. 3 and 4. In these specimens, cation occupancy changed more ordered state by the neutron irradiation, as shown in Fig. 2.

The macroscopic length change and the lattice parameter change of these specimens by the neutron irradiation were measured (Table 1) [23]. The macroscopic length change and the lattice parameter change were small except for the specimen ID44 within the present specimens. The macroscopic length and the lattice parameter of the specimen ID44 increased stepwise by the annealing at around 650 °C, and returned to the pre-irradiation value. The other specimens, ID40, 78 and 113, both length and lattice parameter did not change by the post-irradiation annealing. These changes matched well with the cation distribution changes in the present study. Thus, it is clear that the cation distribution directly related with the macroscopic length and lattice parameter of the present spinel.

All specimens analyzed in this research were prepared through the same process until before the neutron irradiation [22]. On the process of the neutron irradiation, they were put into the same rig and irradiated all together. So there is a large question why the cation distribution of

the specimens (ID40, 78 and 113) was more ordered and that of the other specimen (ID44) disordered after the same level of neutron irradiation in the one irradiation rig, whereas the composition of these specimens were not so largely different. One of the possibilities to induce these modification might be attributed to the 'actual irradiation temperature' of each specimens. The reported irradiation temperature (500–530 °C) is not so far from the order–disorder transition temperature of spinel (~650 °C). There is a possibility that the irradiation close to the transition temperature for long period (440.6 h for the present specimens), affects locally on the cation arrangement of spinel specimens. Further examination is necessary to clarify these uncertainties.

6. Conclusion

The cation distribution of the slightly swelled specimens was ordered by the neutron irradiation. Then, it was changed little by the post-irradiation annealing up to 700 °C. The changes of the macroscopic length and the lattice parameter were little by the annealing as the same tendency with that of cation distribution change. On the contrary, the cation distribution of the contracted specimen was disordered by the neutron irradiation. The cation distribution, the length and the lattice parameter change showed stepwise recovery to the pre-irradiated conditions between annealing at 600–700 °C.

Cation distribution in the T-site was more sensitively influenced by the irradiation. Furthermore, cation vacancies of non-stoichiometric spinel were concentrated in the T-site. The cation vacancies in the slightly swelled specimens were decreased by the neutron irradiation, otherwise they were increased in the contracted specimen. Thus, the O-site in the contracted specimen was overcrowded. That was relaxed after the annealing at 700 °C. This result denoted that the contraction by the neutron irradiation in the spinel specimen was arisen by the disordering of cations.

Acknowledgements

We would like to thank the staff of International Research Center for Nuclear Material Science, Institute for Materials Research, Tohoku University, for their assistance in the irradiation experiment. Thanks are also due for a financial support by a Grant-in-Aid for Scientific Research from the Ministry of Education, Sports, Science and Culture, Japan.

References

[1] N. Kashii, H. Maekawa, Y. Hinatu, J. Am. Ceram. Soc. 82 (1999) 1844.
[2] K.E. Sickafus, J.M. Wills, N.W. Grimes, J. Am. Ceram. Soc. 82 (1999) 3279.
[3] R.L. Millard, R.C. Peterson, B.K. Hunter, Am. Miner. 77 (1992) 44.
[4] S. Hafner, F. Lavcs, Z. Kristallogr. 115 (1961) 321.
[5] H. Cynn, S.K. Sharma, T.F. Cooney, M. Nicol, Phys. Rev. B 45 (1992) 500.
[6] N.V. Minh, I. Yang, Vib. Spectrosc. 35 (2004) 93.
[7] D. Gosset, D. Simeone, M. Dutheil, S. Bouffard, M. Beauvy, J. Eur. Ceram. Soc. 25 (2005) 2677.
[8] N. Ichinosc, Am. Ceram. Soc. Bull. 64 (1995) 581.
[9] E.H. Walker Jr., J.W. Owens, M. Etienne, D. Walker, Mater. Res. Bull. 37 (2002) 1041.
[10] H. Zhang, X. Jia, Z. Liu, Z. Li, Mater. Lett. 58 (2004) 1625.
[11] A. Navrotsky, O.J. Kleppa, J. Inorg. Nucl. Chem. 29 (1967) 2701.
[12] H.S.C. O'Neill, A. Navrotsky, Am. Miner. 76 (1983) 181.
[13] R.C. Peterson, G.A. Lager, R.L. Hitterman, Am. Miner. 76 (1986) 827.
[14] H. Maekawa, S. Kato, K. Kawamura, T. Yokokawa, Am. Miner. 82 (1997) 1125.
[15] T. Soeda, S. Matsumura, C. Kinoshita, J. Zaluzec, J. Nucl. Mater. 283–287 (2000) 952.
[16] B. Hallstedt, J. Am. Ceram. Soc. 75 (1992) 1497.
[17] C.C. Wang, J. Appl. Phys. 40 (1969) 3433.
[18] G.F. Hurley, J.M. Bunch, J. Am. Ceram. Soc. 59 (1980) 456.
[19] F.W. Clinard Jr., G.F. Hurley, L.W. Hobbs, D.L. Rohr, R.A. Youngman, J. Nucl. Mater. 122&123 (1984) 1386.
[20] W.A. Coghlan, F.W. Clinard Jr., N. Itoh, L.R. Greenwood, J. Nucl. Mater. 141–143 (1986) 382.
[21] Y. Fukushima, T. Yano, T. Maruyama, T. Iseki, J. Nucl. Mater. 175 (1990) 203.
[22] T. Yano, Y. Fukushima, H. Sawada, H. Miyazaki, T. Iseki, J. Nucl. Mater. 212–215 (1994) 1046.
[23] T. Yano, H. Sawada, A. Insani, H. Miyazaki, T. Iseki, Nucl. Instrum. and Meth. B 116 (1996) 131.
[24] T. Yano, A. Insani, H. Sawada, T. Iseki, J. Nucl. Mater. 258–263 (1998) 1836.
[25] G.F. Hurley, J.C. Kennedy, F.W. Clinard Jr., J. Nucl. Mater. 103&104 (1981) 761.
[26] T. Zocco, C.D. Kise, J.C. Kennedy, J. Nucl. Mater. 141–143 (1986) 401.
[27] H. Suematsu, T. Iseki, T. Yano, Y. Sato, T. Suzuki, T. Mori, J. Am. Ceram. Soc. 75 (1992) 1742.
[28] C.A. Black, F.A. Garner, R.C. Bradt, J. Nucl. Mater. 212–215 (1994) 1096.
[29] T. Yano, M. Ikari, T. Iseki, E.H. Farnum, F.W. Clinard Jr., T.E. Mitchell, J. Am. Ceram. Soc. 78 (1995) 1469.
[30] L.W. Hobbs, F.W. Clinard Jr., J. Phys. 41 (1980) C6-232.
[31] F.W. Clinard, G.F. Hurley, L.W. Hobbs, J. Nucl. Mater. 108&109 (1982) 655.
[32] C.A. Perker, L.W. Hobbs, K.C. Russell, F.W. Clinard Jr., J. Nucl. Mater. 133&134 (1985) 741.
[33] D.S. Tucker, T. Zocco, C.D. Kise, J.C. Kennedy, J. Nucl. Mater. 141–143 (1986) 401.
[34] K. Nakai, K. Fukumoto, C. Kinoshita, J. Nucl. Mater. 191–194 (1992) 630.
[35] K.E. Sickafus, A.C. Larson, N. Yu, M. Nastasi, G.W. Hollenberg, F.A. Garner, R.C. Bradt, J. Nucl. Mater. 219 (1995) 128.
[36] E.A. Cooper, C.D. Hughes, W.L. Earl, K.E. Sickfus, G.W. Hollenberg, F.A. Garner, R.C. Bredt, Mat. Res. Soc. Symp. Proc. 373 (1995) 147.
[37] J. Taftø, J.C.H. Spence, Science 218 (1982) 49.
[38] J. Taftø, J.C.H. Spence, Ultramicroscopy 9 (1982) 243.
[39] J.C.H. Spence, J. Taftø, J. Microsc. 130 (1983) 147.
[40] S. Lucchesi, A.D. Giusta, Miner. Petrol. 59 (1997) 91.
[41] T. Yamanaka, Y. Takéuchi, Z. Kristallogr. 165 (1983) 65.
[42] P. Fischer, Z. Kristallogr. 124 (1967) 275.
[43] S. Hafiner, F. Laves, Z. Kristallogr. 115 (1961) 321.